Developmental Cell, Vol. 6, 771–780, June, 2004, Copyright ©2004 by Cell Press

Maternal Control of Vertebrate Development before the Midblastula Transition: Mutants from the Zebrafish I

Roland Dosch,[1,2] Daniel S. Wagner,[1,3] Keith A. Mintzer, Greg Runke, Anthony P. Wiemelt, and Mary C. Mullins*
Department of Cell and Developmental Biology
University of Pennsylvania
School of Medicine
1211 BRBII/III
421 Curie Boulevard
Philadelphia, Pennsylvania 19104

Summary

Maternal factors control development prior to the activation of the embryonic genome. In vertebrates, little is known about the molecular mechanisms by which maternal factors regulate embryonic development. To understand the processes controlled by maternal factors and identify key genes involved, we embarked on a maternal-effect mutant screen in the zebrafish. We identified 68 maternal-effect mutants. Here we describe 15 mutations in genes controlling processes prior to the midblastula transition, including egg development, blastodisc formation, embryonic polarity, initiation of cell cleavage, and cell division. These mutants exhibit phenotypes not previously observed in zygotic mutant screens. This collection of maternal-effect mutants provides the basis for a molecular genetic analysis of the maternal control of embryogenesis in vertebrates.

Introduction

Maternally and paternally deposited gene products control embryogenesis prior to the onset of zygotic transcription. In vertebrates, maternal gene products direct fertilization, egg activation, the first cell division(s), and the initiation of zygotic transcription. Additionally, maternal factors act in the determination of the body axes (reviewed in Moody et al., 1996; Moon and Kimelman, 1998). In amphibians and fish, the animal-vegetal (AV) or prospective anterior-posterior axis is established during oogenesis, as apparent from the asymmetric localization of the germinal vesicle and specific mRNAs (Bally-Cuif et al., 1998; Howley and Ho, 2000; Maegawa et al., 1999; Suzuki et al., 2000; reviewed in King et al., 1999). The dorsal-ventral axis is established during early embryonic cleavage stages and also relies on maternal gene products (reviewed in De Robertis et al., 2000; Schier, 2001). Thus, maternal factors in lower vertebrates provide the foundations for embryonic development, which zygotic factors build upon later.

*Correspondence: mullins@mail.med.upenn.edu
[1]These authors contributed equally to this work.
[2]Present address: Departement de Zoologie et biologie animal, Universite de Geneve, Sciences III, 30 quai Ernest-Ansermet, CH-1211 Geneve, Switzerland.
[3]Present address: Department of Biochemistry and Cell Biology, Rice University, MS-140, PO Box 1892, Houston, Texas 77251.

In the mouse, maternal factors also play a role in embryonic development. Since the zygotic genome is not active before the 2-cell stage in the mouse (reviewed in Schultz, 1993), the first cell division depends on maternal gene products. Moreover, the AV axis of the mouse embryo is established during oogenesis and the future body axes of the embryo may be evident at fertilization (Gardner, 2001; Piotrowska and Zernicka-Goetz, 2001). A role for maternal factors in mammalian embryonic development is demonstrated by several maternal-effect mutations in the mouse (Burns et al., 2003; Bourc'his et al., 2001; Christians et al., 2000; Gurtu et al., 2002; Howell et al., 2001; Leader et al., 2002; Payer et al., 2003; Tong et al., 2000; Wu et al., 2003).

To study processes controlled by maternal factors in vertebrate development and to identify key genes mediating these processes, we conducted a systematic, recessive maternal-effect mutant screen in the zebrafish. We identified 68 maternal-effect mutants, about half of which displayed specific abnormalities. Here we describe 15 mutations that affect embryogenesis prior to the onset of zygotic transcription, such as egg development, blastodisc formation, animal-vegetal polarity, and cell cleavage. Together with the mutants in the accompanying paper (Wagner et al., 2004), this collection of vertebrate maternal-effect mutants provides an important tool to dissect the cellular and molecular mechanisms under maternal control in vertebrate development.

Results and Discussion

A Four-Generation Maternal-Effect Mutant Screen

To systematically isolate maternal-effect mutations in the zebrafish, we designed a four-generation natural crossing strategy (Figure 1A), rather than following a previous three-generation "early-pressure" gynogenetic strategy (Pelegri et al., 1999; Pelegri and Schulte-Merker, 1999). The natural crossing strategy required an extra generation and yielded a lower fraction of homozygous females within a family than the gynogenetic method, but combines three advantages. (1) We could use a higher dose of the chemical mutagen, N-ethyl-N-nitrosourea (ENU) in the natural crossing strategy, resulting in a higher mutation rate. With the gynogenetic method, a lower ENU dose was used to increase survival to adulthood, since fewer embryos survive the early pressure treatment itself and the widespread homozygosity of zygotic lethal-induced mutations reduces viability further (Pelegri and Schulte-Merker, 1999). (2) The gynogenetic strategy is biased against loci located distal from a centromere, because of the increased probability of meiotic recombination (Postlethwait and Talbot, 1997; Streisinger et al., 1981). (3) Most importantly, the four-generation crossing strategy allowed us to implement a mapping cross within the screen, which is critical to maintain efficiently the mutant lines and identify the mutated genes (Figure 1B).

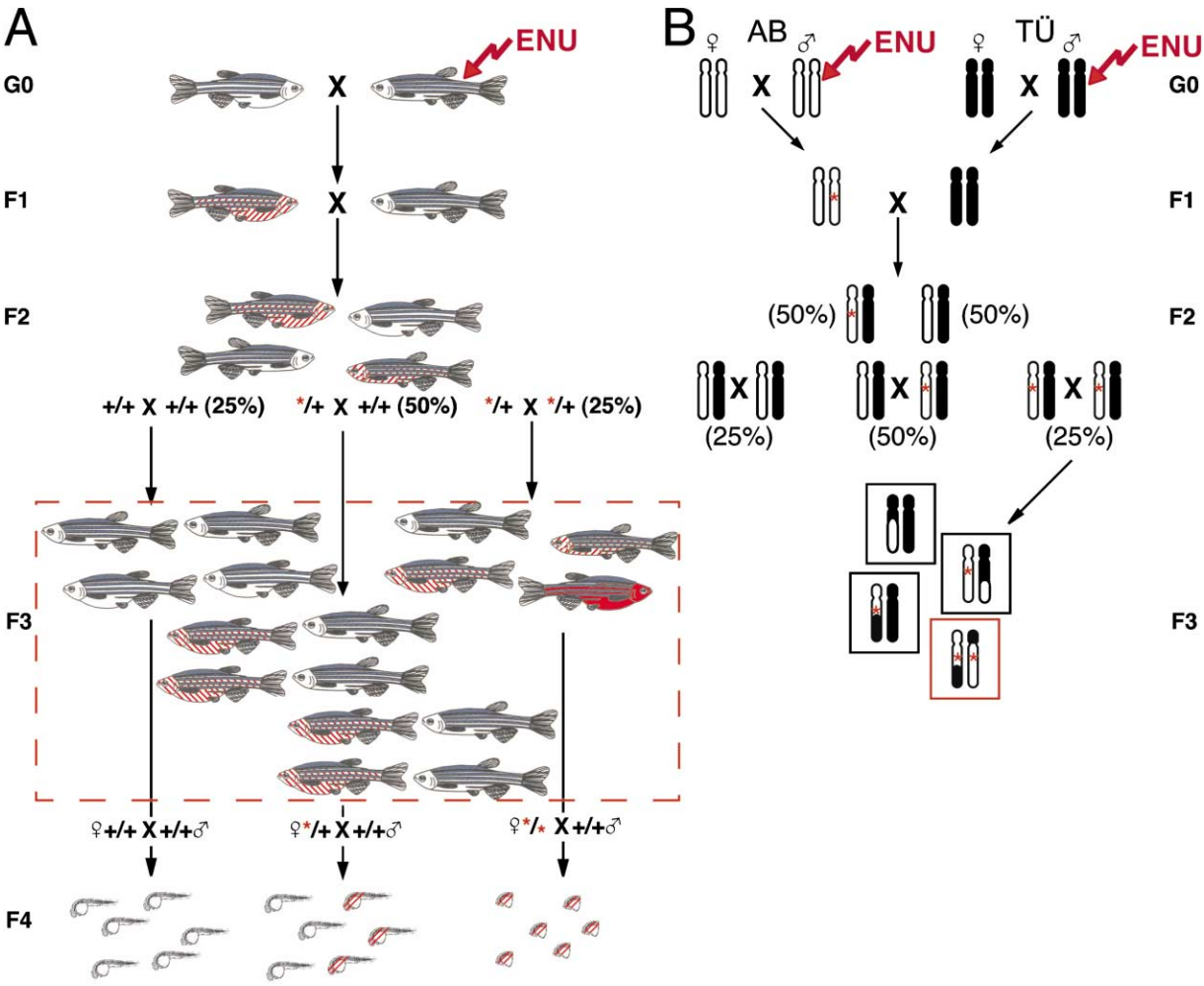

Figure 1. A Four-Generation Crossing Strategy to Isolate and Map Maternal-Effect Mutations in the Zebrafish

(A) Mutagenized G0-males were crossed to wild-type females. Each resultant F1-fish is heterozygous for a different set of induced mutations, but for simplicity only one mutation is depicted (symbolized by red stripes). F1-fish were intercrossed to generate F2-families, in which 50% of the fish were heterozygous for each induced mutation. Each F2-family contains two mutagenized genomes, one derived from each F1 parent. The F2-fish within a family were randomly intercrossed. 25% of these crosses are expected heterozygote intercrosses (*/+ x */+, red asterisk indicates the mutation), yielding 25% homozygous F3-offspring for an induced mutation (solid red fish). Heterozygous intercrosses cannot be identified a priori. Therefore, to use aquarium space efficiently, we pooled equal numbers of F3-progeny from an average of 15 individual F2-crosses, raising an "F3-extended family" of siblings and cousins in a single tank (dashed red box). 6.25% of females in this extended family should be homozygous for a given mutation (solid red fish). To obtain an ~80% probability of identifying at least one mutant female, 25 females were screened from each F3-family (see also Experimental Procedures). The F4-progeny of the F3-females were screened at 1 dpf for survival and morphological defects (see Experimental Procedures).

(B) To facilitate propagation of the mutant lines, we implemented a mapping cross in the screen strategy, as symbolized by the chromosome schematics. G0-males from the AB-strain (white chromosomes) and TÜ-strain (black chromosomes) were mutagenized and crossed to females of the same strain to generate heterozygous fish in the F1-generation (red asterisk indicates one maternal-effect-induced mutation in an AB fish). In the F1-generation, fish from the TÜ- and AB-strain were intercrossed to generate hybrid F2-families, whereby each F2-fish carries one set of chromosomes from TÜ and one from AB. Individual F3-families were regenerated (not an F3-extended family) from single pairs of F2-fish to obtain sufficient mutant females to perform bulk segregant analysis. A quarter of the F2-intercrosses will be between heterozygotes, yielding 25% F3 homozygous maternal-effect mutant females (red box). F3 mutant females are homozygous for AB-derived loci in the region of the mutation, whereas other chromosomes in the mutant pool are a mixture of AB and TÜ (not shown).

Using the four-generation crossing strategy, we generated 400 F3-families, each of which carried two independently mutagenized genomes (Figure 1). To identify maternal-effect mutants, F3-females were crossed to either sibling or wild-type males and their F4-embryos screened for survival and morphological defects visible at 1 dpf (see also Figure 1 and Experimental Procedures). We screened 600 mutagenized genomes and identified 68 maternal-effect mutants. Mutants manifesting their phenotypes before the midblastula transition are described here, whereas those first visible at or after the midblastula transition are described in Wagner et al. (2004, this issue). Since the term "maternal-effect mutation" applies to a mutation affecting the embryonic development of progeny from a mutant mother, some of the mutations described here likely

Table 1. Maternal-Effect Mutants with Phenotypes before the Midblastula Transition

Class	Number of Mutants Identified	Genes/Alleles	Chromosomal Location
Opaque egg	4	*ruehrei*^{p25ca}	Chr 6 (z9738/z5294)
		over easy^{p37ad}	ND
		sunny side up^{p144dc}	Chr 22 (z230/z26264)
		souffle^{p96re}	Chr 13
Egg activation and cytoplasmic segregation	5	*jumpstart*^{p108re}	ND
		p11cv	ND
		emulsion^{p41pj}	Chr 4 (z11876/z7496)
		dp14nb	
Animal-vegetal polarity	2	*bucky ball*^{p106re}	ND
		p6cv	ND
Failure to initiate cleavage	3	*atomos*^{p71fm}	Chr 9 (z64472/telom.)
		indivisible^{p15dia}	ND
		irreducible^{dp15mf}	Chr 20 (z536/telom.)
Incomplete cellularization	7	*cellular island*^{p63cd}	ND
		cellular atoll^{p37mfa}	Chr 22 (z10673/z4284)
Male sterile	20	*shooting blanks*^{p12cdc}	ND

"Number of mutants identified" indicates total number of mutants found in the class. "Genes/Alleles" lists only the lines that were propagated. Gene names were given to alleles that have either been mapped to a chromosomal position or excluded from linkage to other mutations in the same class. An allele designation without a gene name indicates that the mutation has not been excluded as allelic to another gene in the class. ND, not determined. Dominant mutations begin with a "d" in their allele designation.

represent female sterile mutations, since a defect in the oocyte or egg may preclude zygote formation and hence block the progression of embryogenesis. All the mutant defects described below are strict maternal-effect phenotypes, and all embryos or eggs in the analyses that follow are derived from mutant females crossed to wild-type males.

A group of 21 mutants displayed defects prior to the midblastula transition and, of these, 15 representative lines were kept and propagated. All of these mutants exhibit phenotypes not previously observed in zygotic mutant screens. Nearly all display fully penetrant, uniform phenotypes. These mutants were placed into five phenotypic classes (Table 1). For simplicity, we will refer to the embryos derived from the homozygous maternal-effect mutant females as mutant embryos.

Opaque Egg Mutants

During stage IV of oogenesis, the oocyte matures and its appearance changes from opaque to transparent (Selman et al., 1993). In four maternal-effect mutants, *over easy* (*ovy*^{p37ad}), *ruehrei* (German for "scrambled eggs", *rei*^{p25ca}), *sunny side up* (*ssu*^{p144dc}), and *souffle* (*suf*^{p96re}), we observed opaque rather than transparent eggs (Table 1, Figures 2A–2F). These eggs also fail to segregate cytoplasm to the animal pole to form the blastodisc, which normally occurs during egg activation. The appearance of these mutant eggs is similar to that of prematurational stage IV oocytes (Figure 2B), suggesting a defect in oogenesis.

During stage IV of oogenesis, the composition of major yolk proteins changes (Selman et al., 1993). Using Coomassie-stained SDS-gels, we compared the composition of the major yolk proteins from stage V opaque egg mutants to immature stage IV oocytes and stage V eggs from wild-type sibling mothers. We found that mutant eggs displayed more of the larger molecular weight yolk protein, similar to wild-type immature stage IV oocytes (Figure 2G). All other protein bands between mutants and wild-type appeared identical, with the exception of one protein band in *sunny side up* eggs of about 28 kDa (Figure 2G and data not shown). In summary, opaque egg mutants showed similarities to immature oocytes in their morphological phenotype and in their composition of major yolk proteins.

The opaque egg mutants also showed no cellular cleavages. To address whether nuclear division occurred in these mutants, we stained them with the DNA-dye DAPI. We found that some *over easy* (26%, n = 47) and all *ruehrei* and *sunny side up* mutants exhibited multiple spots of DAPI-stained chromatin at one pole of the egg (Figures 2H and 2I), whereas most *over easy* (74%) and all *souffle* mutants displayed a single nucleus (data not shown).

The opaque egg mutants may represent a defect in progression through oocyte maturation during stage IV of oogenesis. The *over easy* and *souffle* mutants are currently the best candidates for the earliest defect, exhibiting the opaque color and yolk protein profile of immature stage IV oocytes, and a lack of nuclear divisions. Oocyte maturation has been intensively investigated in amphibian oocytes (reviewed in Nebreda and Ferby, 2000). However, when mutated, few of the genes implicated in these studies cause an oocyte maturation defect (Colledge et al., 1994; Hashimoto et al., 1994; Tay and Richter, 2001; Lincoln et al., 2002). One or all of the opaque egg mutant genes may be members of a pathway required for oocyte maturation in vertebrates.

Defective Egg Activation and Cytoplasmic Segregation Mutants

Immediately following egg laying, the zebrafish egg is activated by release of the egg into a hypotonic environment. Egg activation includes fusion of the cortical granules to the egg membrane and release of their contents, resulting in expansion and hardening of the chorion (reviewed in Hart, 1990). The zebrafish egg also changes

from somewhat flat and oblong to round, and the cytoplasm, initially integrated within the yolk, segregates to the animal pole to form the blastodisc.

In *jumpstart* (*jum*^{p108re}) and *p11cv* mutants, some of these processes do not occur and the embryos resemble eggs before activation (Figures 3A–3C, data not shown). Many of the eggs are flat and oblong and the blastodisc is a small crescent. In time-lapse microscopy analysis of *jumpstart* mutant eggs, we did not detect cytoplasmic segregation movements or cellular cleavages (data not shown). We examined the cortical granules in *jumpstart* mutants with MPA (*Maclura pomifera* agglutinin) (Becker and Hart, 1999). In *jumpstart* mutant eggs, cortical granule release proceeded but was not complete, and large patches remained at 30 mpf, unlike wild-type eggs (Figures 3D–3F). Thus, several aspects of egg activation, including changes in egg morphology, cortical granule exocytosis, and cytoplasmic segregation, are not fully executed in *jumpstart* mutant eggs.

Two mutants, *dp14nb* and *emulsion* (*emn*^{p41pj}), displayed defects in a specific aspect of egg activation, the segregation of cytoplasm from the yolk to the blastodisc. In the *emulsion* mutant, less cytoplasm segregates to the blastodisc and the interface between the yolk and cytoplasm is less distinct than in wild-type (Figures 3G and 3I). The yolk is grayish and the yolk vesicles are more evident in the mutants than wild-type, likely reflecting the incomplete segregation of the cytoplasm from the yolk. Cell cleavages initiate, but then fail in most mutants, such that by sphere stage ($\sim$1 hr post MBT) only 35% of the mutants were cellularized with an obvious reduced size of the blastoderm. Only 30% (n = 596) of these cellularized mutants survived to 1 dpf and all exhibited a body axis of reduced size to varying degrees (Figures 3H and 3J), likely due to the small size of the blastoderm. We conclude that the *emulsion* mutant is defective in cytoplasmic segregation following egg activation. Since microfilaments are required for cytoplasmic segregation (Hart and Fluck, 1995; Leung et al., 2000), microfilament function may be defective in this mutant. Together, the four maternal-effect mutants we identified may provide molecular-genetic means of dissecting the process of egg activation in vertebrates.

Animal-Vegetal Polarity Mutants

The polarity of cytoplasmic streaming causes the blastodisc to form specifically at the animal pole. In the *bucky ball* (*buc*^{p106re}) and *p6cv* mutants, the cytoplasm segregated radially around the circumference of the yolk and subsequent cellular cleavages did not occur (Figures 3K and 3N and data not shown). In the *bucky ball* mutant, cytoplasmic streaming was evident in multiple orientations, rather than in a single orientation toward the animal pole as in wild-type, suggesting a defect in animal-vegetal polarity of the egg.

To investigate the animal-vegetal polarity phenotype of *bucky ball* mutant eggs, we examined the localized mRNAs *cyclinB* (Kondo et al., 1997) and *bruno-like* (Howley and Ho, 2000; Suzuki et al., 2000). The *cyclinB* mRNA, which is normally localized to the animal pole of the egg, extended around the circumference of the mutant

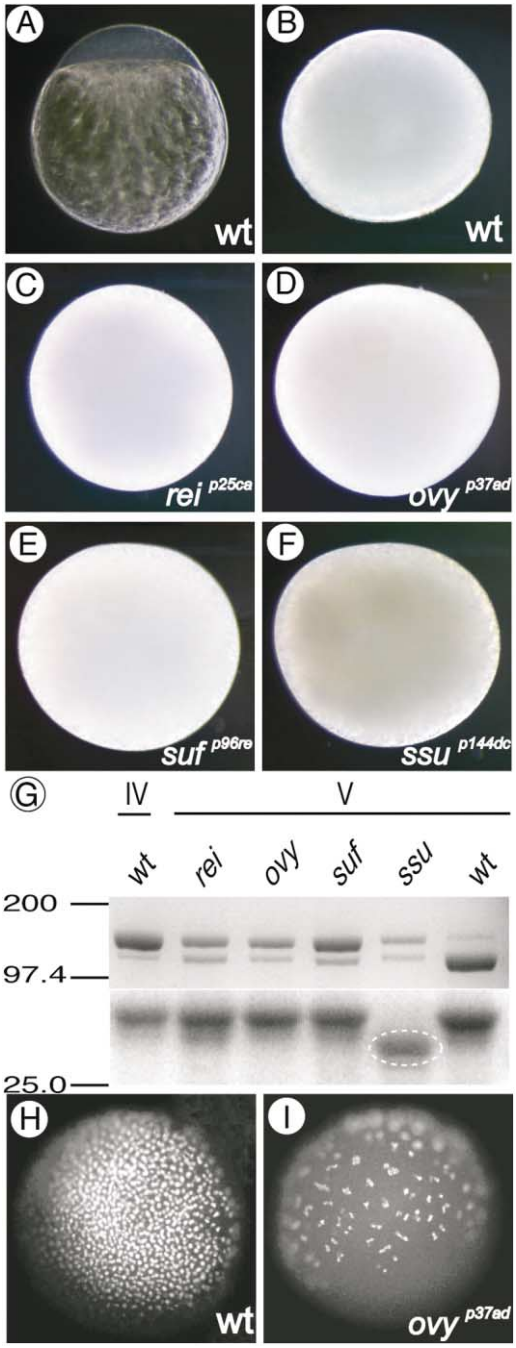

Figure 2. Opaque Egg Mutants

(A–F) Live wild-type embryo at 30 mpf (A), and a stage IV oocyte (B) in incident light. Opaque egg mutants 30 mpf, (C) *ruehrei*, (D) *over easy*, (E) *souffle*, and (F) *sunny side up*.

(G) Coomassie-stained SDS-PAGE of major yolk proteins of stage IV oocytes from wild-type females (wt) and stage V eggs from the opaque egg mutants and wild-type sibling females of the *ssu* mutant. Note in the upper gel the preponderance of the high molecular weight band in mutant eggs and wild-type stage IV oocytes, whereas the lower molecular weight band predominates in wild-type eggs. The amount of protein in each lane of the upper panel corresponds to 10% of an egg, whereas the lower panel corresponds to one egg equivalent (white dashed oval, 28 kDa protein present in *ssu*).

(H and I) Nuclear stain (DAPI) in an animal view of a wild-type embryo at sphere stage (midblastula) (H) and lateral view of an age-matched *ovy* mutant (I).

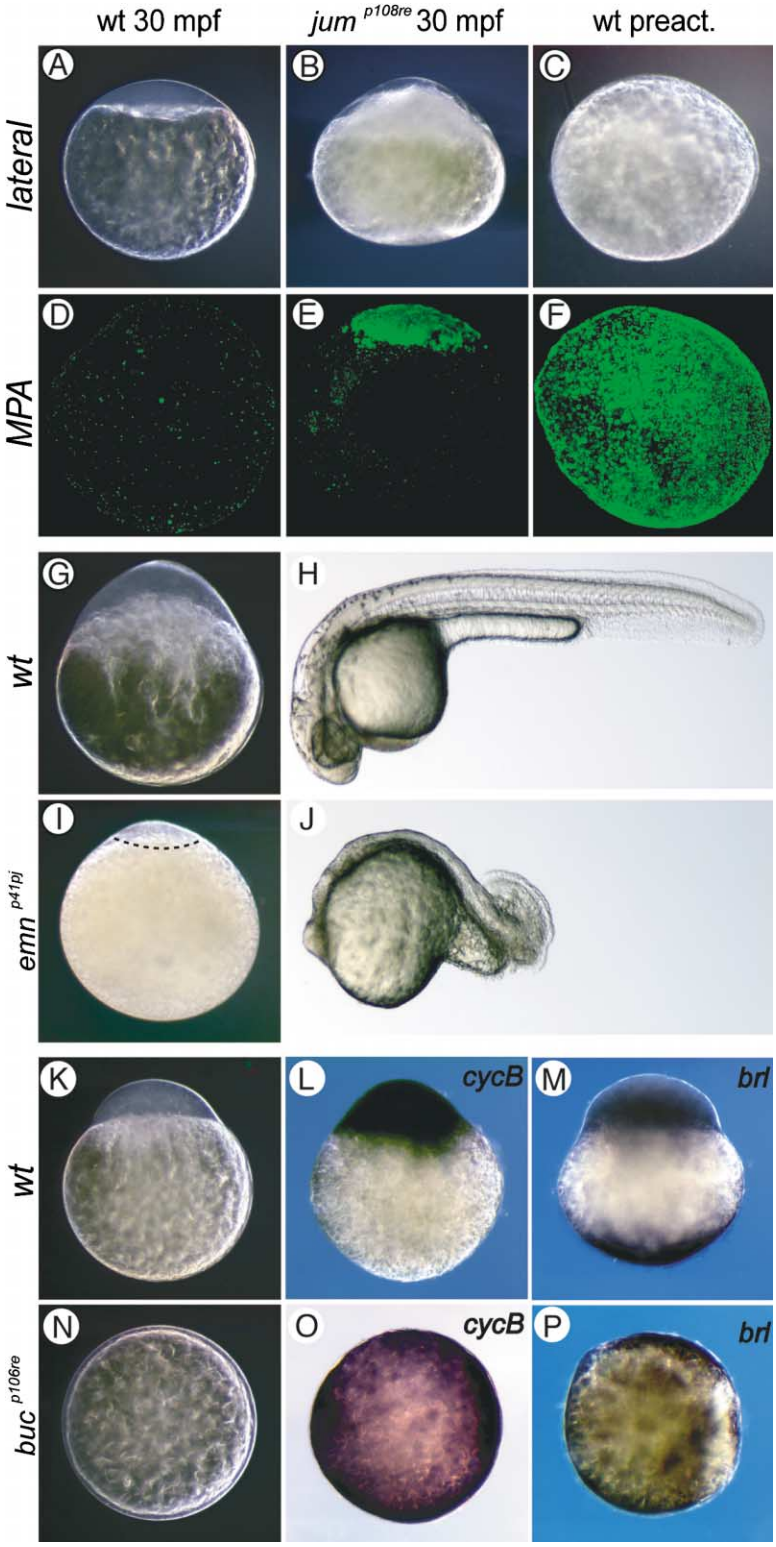

Figure 3. Egg Activation, Cytoplasmic Segregation, and Animal-Vegetal Polarity Mutants

A wild-type embryo (A), a *jumpstart* mutant (B), and an unactivated wild-type egg (C). (D–F) Confocal images of cortical granules stained with MPA in green in 30 mpf wild-type (D) and *jumpstart* ([E], note the patch of cortical granules) embryos, as well as eggs before activation (F). Wild-type embryo 30 mpf (G) and at 30 hpf (H). *emulsion* mutant embryos at 30 mpf ([I], black dashed line is the small blastodisc) and 30 hpf (lateral view, anterior to left). Wild-type embryo, cytoplasm to the animal pole (K). Whole-mount in situ hybridization in wild-type embryo of *cyclinB* (*cycB*) (L) and *bruno-like* (*brl*) (M) mRNA. *bucky ball* (*buc*) mutant embryos develop a halo of cytoplasm around the circumference of the yolk (N). In *buc* embryos, *cycB* (O) and *brl* (P) mRNA are not localized. (A–C, G, I, K, and N) Live eggs in incident light, lateral views, animal to the top.

(Figures 3L and 3O). The *bruno-like* mRNA, which localizes to the vegetal pole during oogenesis and then to both animal and vegetal poles following egg activation, was not localized in the mutant (Figures 3M and 3P). Since mRNA at both the animal and the vegetal pole is unlocalized, the animal-vegetal axis appears disrupted, rather than an animal- or vegetal-specific RNA localization mechanism. In summary, the phenotype and mislocalization of mRNA in the *bucky ball* mutant suggest a defect in embryonic polarity along the animal-vegetal axis.

Mutants that Fail to Initiate Cell Cleavage

Forty-five minutes after fertilization, the blastodisc initiates cell cleavages. Three mutants, *irreducible* (*irr*^{dp15mf}), *indivisible* (*ini*^{p15dia}), and *atomos* (*aoo*^{p71fm}) appeared similar to unfertilized eggs, failing to initiate both cytokinesis and karyokinesis (Figures 4A–4D). To distinguish between a defect in fertilization or the initiation of cell cleavage in the *indivisible* mutant, we tested whether sperm DNA could be isolated from mutant embryos. We crossed mutant and wild-type control females to males carrying a GFP-transgene (Pauls et al., 2001) and then examined if the sperm-DNA was present in the egg by transgene-specific PCR. As Figure 4E shows, paternal DNA was present in wild-type and mutant eggs, suggesting that *indivisible* eggs are fertilized, but do not initiate cleavage.

To test if the sperm fertilizes the egg, rather than just adheres to it, we examined male pronucleus formation. Eggs were fertilized in vitro and fixed at 10 mpf, before the male and female pronuclei fuse (Dekens et al., 2003). In 69% (n = 29) of the wild-type eggs, we detected three nuclei, two produced by the female pronucleus undergoing the second meiotic cleavage and one representing the male pronucleus (Figure 4F). The observed number of eggs with three nuclei correlates with the fertilization rate of the nonfixed control sample (70%). In 21% (n = 42) of the mutant eggs, we also found three nuclei (Figure 4G), demonstrating that the sperm can fuse with *indivisible* eggs. However, none of the mutant eggs from the nonfixed control sample initiated cleavage. These results indicate that sperm can fertilize *indivisible* mutant eggs but that cell cleavage does not initiate. The defects in the other two cleavage initiation mutants may originate from a failure to complete meiosis, a lack of fertilization, or a block to the initiation of the first cell cycle.

Incomplete Cellularization Mutants

A group of seven mutants showed cleavage furrow ingression during the initial cleavages following fertilization, but after several rounds of cell division, cytokinesis failed, while karyokinesis continued. In the two representative mutants of this class, *cellular island* (*cei*^{p63cd}) and *cellular atoll* (*cea*^{p37mf}), many of the embryos developed pockets of normal appearing blastomeres surrounded by clear cytoplasm (Figures 4H and 4L and data not shown). We found that the acellular regions in both mutants exhibited a multitude of DAPI-positive nuclei, indicating that the nuclei divide in the acellular regions (Figures 4J and 4N and data not shown). To investigate the cellular structure of the blastoderm in *cei* mutants, we examined cell membrane localization of β-catenin and nuclei with DAPI. We found that the cellularized areas displayed normal nuclei and cell membranes, whereas the acellular regions showed clumps of nuclei, indicating that nuclear division, but not cytokinesis, occurred in these regions (Figures 4I–4K and 4M–4O). In time-lapse microscopy analysis, the nuclei of *cei* mutants divided in synchrony, similar to wild-type nuclei at these stages (see Supplemental Data at http://www.developmentalcell.com/cgi/content/full/6/6/771/DC1). These cytokinesis mutants look similar to the zebrafish maternal-effect mutant, *nebel*, which is defective in the formation of new cellular membranes (Pelegri et al., 1999).

To examine if the *cei* nuclei could respond to inductive signaling events and activate transcription, we examined the expression of the mesodermally restricted gene *no tail* (*ntl*)/*brachyury*, which normally is expressed in marginal blastomeres in response to a yolk-cell-derived mesoderm inducing signal (reviewed in Schier, 2001). We found that the cellularized nuclei could activate *ntl* gene expression, whereas the uncellularized areas of the embryo could not (Figures 4P and 4Q). Cellularization may be crucial for the transduction of a mesoderm-inducing signal, such as the Squint and Cyclops Nodal-related ligands (Feldman et al., 1998; Rebagliati et al., 1998; Sampath et al., 1998), and consequently uncellularized *cei* nuclei cannot respond.

Interestingly, cellularized regions in the *cei* mutant located more distant from the margin than the wild-type *ntl* expression domain could initiate *ntl* expression in the mutant (Figures 4P and 4Q); however, there was a limit to this distance and animal pole cellularized patches could not initiate *ntl* expression (data not shown). Mesoderm forms only at the margin due to the presence of a mesoderm-inducing factor restricted to the yolk syncytial layer (YSL) (Chen and Kimelman, 2000; Mizuno et al., 1996; Ober and Schulte-Merker, 1999). In *cei* mutants, the large nuclear syncytium that forms may take on the characteristics of the YSL, thus inducing ectopic mesoderm. Alternatively, a mesoderm-inducing factor may more freely traverse the nuclear syncytium, where cell membranes and their constituents do not impede movement, thus causing ectopic mesoderm induction.

Male-Sterile Mutants

Although we did not specifically screen for defects in males, we found 20 male sterile mutants (see Experimental Procedures). To address the cellular basis for this defect in the mutant *shooting blanks* (*shb*^{p12cdc}), we investigated its sperm microscopically. We did not find any obvious morphological defects or a lack of sperm. To examine the motility of the *shooting blanks* sperm, we activated it by the addition of water. We found that sperm of *shooting blanks* males remained immotile after activation, whereas control sperm became motile (Figures 4R–4U and Supplemental Data). Both wild-type and mutant sperm retracted their tails after activation, indicating that the mutant sperm are capable of activation in this assay. We conclude that the male sterile phenotype of *shooting blanks* is caused by a defect in sperm motility.

Mapping and Propagating the Maternal-Effect Mutations

In contrast to zygotic mutants, it is more challenging to propagate a maternal-effect mutation by standard crossing methods in vertebrates. Since most homozygous maternal-effect mutant females produce only nonviable offspring, it is necessary to identify heterozygous carriers or homozygous males to maintain the mutant line. To obviate continued use of a laborious, random two-generation intercrossing strategy to identify heterozygous carriers, we incorporated a mapping cross into the mutagenesis crossing scheme (Figure 1B). This

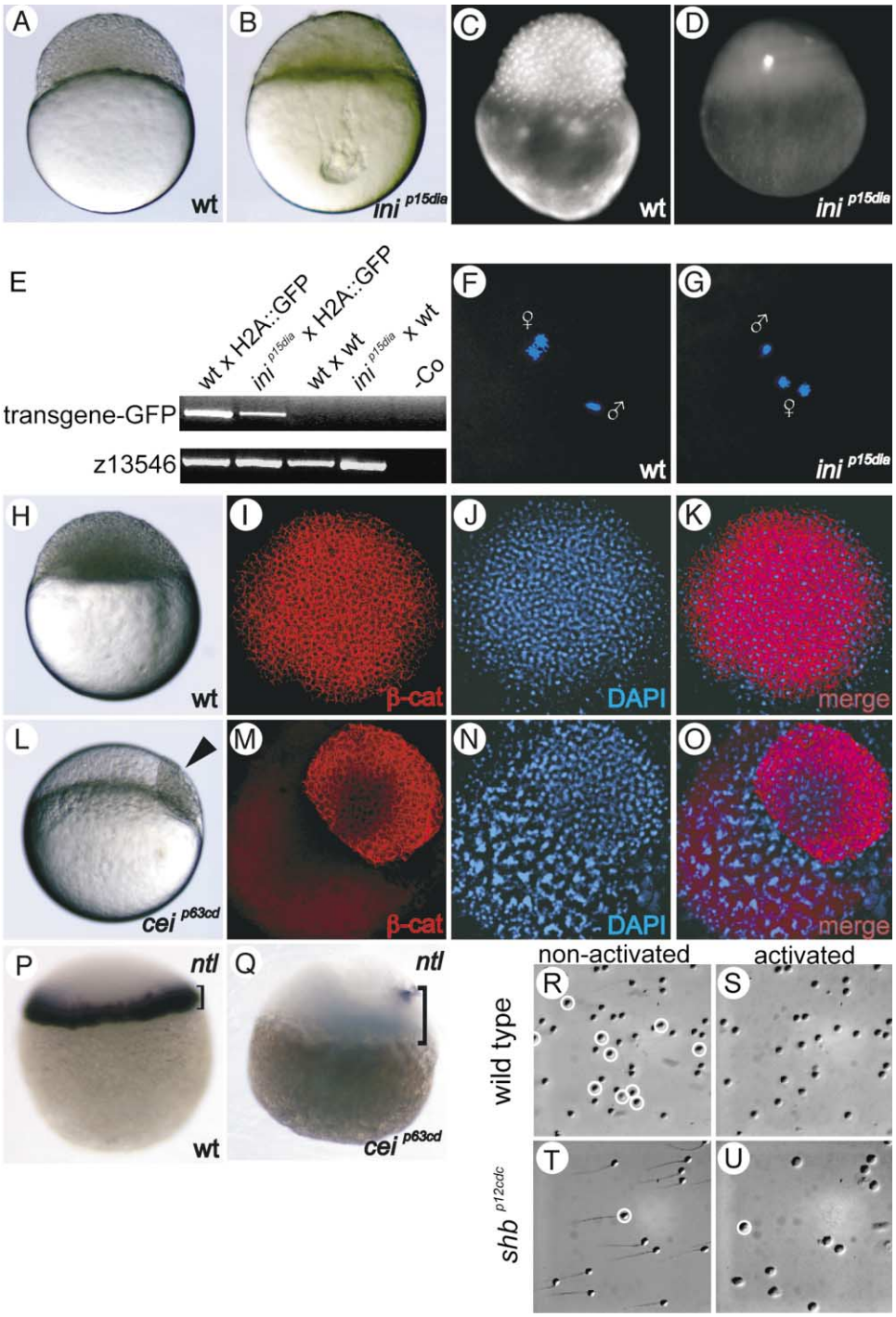

Figure 4. No Cleavage, Partial Cleavage, and Male Sterile Mutants

A wild-type blastula (high stage) (A), and age-matched *ini* embryo that fails to initiate cleavage (B). DAPI-staining at this stage shows numerous, small nuclei in wild-type (C), whereas the *ini* mutant exhibits one large nucleus (D), similar to unfertilized eggs (data not shown). (E) Fertilization assay. A paternally derived GFP-transgene (H2A::GFP) detected by PCR in wild-type, as well as *ini* mutant embryos at 3 hpf, but not in embryos fertilized with nontransgenic, control sperm (wt). The presence of the z13546 marker confirmed the presence of genomic DNA in all samples, except the non-DNA-containing control (-Co).

(F and G) Detection of the male pronucleus in *ini* mutants at 10 mpf with DAPI.

(H–Q) Partial cleavage *cellular island* (*cei*) mutant. Wild-type embryo live (H), and stained for β-catenin (I) and DAPI (J), and merged in (K). *cei* mutant embryo live with a cellularized pocket (arrowhead) in a clear acellular blastoderm (L), and stained for β-catenin (M) and DAPI (N), and merged in (O). The clumping of nuclei in the acellular regions of *cei* mutants is typical of cytokinesis defects (Sullivan et al., 1993). (P and Q) Whole-mount in situ hybridization at 50% epiboly shows *no tail* (*ntl*) expression only in the cellularized area of the blastoderm (brackets indicate the distance from the yolk margin to the animal-most extent of the *ntl* expression). Lateral views (A–D, H, L, P, and Q), animal views (I–K, M–O). Confocal images (F, G, I–K, M–O).

Unactivated, immotile, and activated sperm from wild-type (R and S) and the *shb* mutant (T and U). White circles in (R) indicate sperm heads that left the field of view after activation. The single marked *shb* sperm (T and U) moved due to passive drifting after water addition.

allows us to directly map the mutation to a chromosomal location from F3 mutants and identify carriers by a PCR-based genotyping method. Using this strategy, it was necessary to perform only one generation of random F2-intercrosses to identify F2-heterozygotes, which were then bred to obtain sufficient numbers of F3 mutant females to map the mutation (see Experimental Procedures).

We scanned the genome for linkage of the maternal-effect mutations to about 170 simple-sequence-length-polymorphic (SSLP) markers and mapped seven mutations (Table 1, Supplemental Data, and data not shown). We found that the *emulsion* mutation is located on chromosome 4. The failure-to-cleave mutations, *atomos* and *irreducible*, are located on chromosome 9 and 20, respectively. The *cellular atoll* mutation causing incomplete cellularization is on chromosome 22. Lastly, we mapped three of the mutations causing the opaque egg phenotype, *ruehrei*, *souffle*, and *sunny side up*, which are located on chromosomes 6, 13, and 22, respectively. Using SSLP markers flanking the *sunny side up* and *ruehrei* mutations, we identified heterozygous females and homozygous mutant males and propagated the mutant lines into the next generation. In all subsequent generations, we can continue to use these PCR-based markers to identify carriers, propagate the strain, and more finely map the mutations to identify the affected genes.

We used the chromosomal positions of the mapped mutations to test if other mutations in the same phenotypic class are mutant alleles of the same gene or independent genes. The mapped mutations represent four different phenotypic classes. We examined linkage of the nonmapped mutations in a class to the position of the mapped mutation(s). We found that the fourth mutation causing an opaque egg phenotype, *over easy*, is not linked to the position of the *sunny side up*, *souffle*, or *ruehrei* mutations (data not shown), demonstrating that it is an independently mutated gene. For the failure to initiate cleavage class, we found that the *indivisible* mutation is not linked to the position of the *irreducible* or *atomos* mutations (data not shown). Similarly, we found that the *cellular atoll* mutation is not linked to *cellular island*. Thus three mutant classes are composed of two to four independently mutated genes, yielding the promise of identifying multiple components of pathways acting in similar processes.

We predict that after screening 600 genomes, the vast majority of mutations would represent alterations in independent genes and a handful would have more than one allele, based on similar findings from one of the large-scale zygotic mutant screens in zebrafish (M.C.M., unpublished data). Consistent with this expectation, the 11 mutations examined so far all correspond to different mutated genes. Thus, our screen successfully identified genes likely encoding multiple molecular components in several specific maternally controlled processes, which was our goal.

Conclusion

Mutants provide a crucial tool to investigate the role of genes in a biological process. Moreover, collections of mutants in a process can be key to elucidating the molecular mechanisms or pathways controlling this process. We have used this approach to study the role of maternal gene products in vertebrate embryonic development. Here we described 15 maternal-effect mutations, which cause defects in genes that control developmental processes prior to the midblastula transition, including oocyte development, blastodisc formation, embryonic polarity, and cell division. Recent evidence shows that some zygotic transcription occurs prior to the midblastula transition in *Xenopus* (Kimelman and Kirschner, 1987; Yang et al., 2002), leaving open a role for some zygotic control of early cleavage stage processes. Our mutants provide us with definitive control steps that require maternal regulation in the zebrafish prior to, as well as following the midblastula transition (see also Wagner et al., 2004, this issue). Moreover, many of the processes that are defective in these mutants are also under maternal control in mammals. The mutants identified provide key molecular-genetic entry points to a wide range of developmental processes, many not previously represented in zebrafish or other vertebrates, possibly identifying new roles for previously known genes and novel genes.

Experimental Procedures

Fish Breeding, Mutagenesis, and Screening for Embryonic Phenotypes

Males of the TÜ and AB strains were mutagenized with 3.3 or 3.0 mM ENU essentially as described (Mullins et al., 1994). Mutagenized males were crossed on alternate weeks to females of the same strain or females double mutant for *golden* and *sparse*. The average noncomplementation rates for all mutagenized fish were 0.12% for *golden* and 0.14% for *sparse*, as published (Mullins et al., 1994; Solnica-Krezel et al., 1994).

To calculate the genomes screened in a single F3 family, we used the following formula: $G=(1\text{-}0.9375^{n})\times(2\times(1\text{-}0.75^{m}))$, where G is the genomes screened; 0.9375 represents the probability of identifying an F3 wild-type female in one cross from the F3-extended family—because we pooled equal numbers of F3 embryos from multiple F2 intercrosses of one family, making an F3-extended family (see Figure 1), wild-type females are found at 93.75%, rather than 75% frequency; "n" is the number of females screened in a particular F3 family; $(1\text{-}0.9375^{n})$ then indicates the probability of identifying a recessive F3 maternal-effect mutant female if "n" females are screened in an F3 family; "2" represents the two mutagenized genomes derived from the two F1 fish. $(1\text{-}0.75^{m})$ calculates the portion of the two mutagenized genomes found in the F2 generation that are transmitted to the F3 generation; (1-0.75) is the probability that in a single F2 cross, two heterozygous carriers of a maternal-effect mutation were crossed together to generate homozygous mutants; and "m" is the number of F2-crosses performed. The value of G was calculated for each of the 398 families screened and summed, giving a total of 605 genomes screened.

To identify maternal-effect mutants, F3 females were crossed to sibling/cousins or wild-type males. F4-embryos were screened at 1 dpf for morphological defects and survival. Typically, if more than 35% of embryos were affected and less than 15% of the F3-intercrosses showed the phenotype, we considered the mutation a potential maternal-effect mutation, rather than a recessive zygotic mutation. We then retested the same pair of fish in an intercross. If an F3 intercross retested positive, then the F3-female and male were separately crossed to wild-type fish of the TLF-strain, to determine if the father (paternal-effect), the mother (maternal-effect) or both (maternal-zygotic) caused the mutant phenotype. This procedure also allowed us to identify recessive paternal-effect and male-sterile mutants. We identified no maternal-zygotic mutants in our screen. A female was considered to be a maternal-effect mutant if she

generated a uniform and reproducible mutant phenotype in her offspring, when crossed to a wild-type male.

To map a mutation to a chromosomal position, a dozen or more mutant females were desired for bulk segregant analysis. In the original F3-extended family, between one and five mutant females were identified. To generate sufficient females for mapping purposes, we kept ten pairs of F2-fish from each family. Individual F3-families were regenerated from single pairs of F2-fish, raised in separate tanks, and screened for mutants (not pooled as in the original F3-family screened). Thus, heterozygous F2-fish were identified by the presence of mutant females in their offspring. The F2-heterozygotes were then subsequently bred, if necessary, to obtain sufficient numbers of mutants for mapping.

To determine the first appearance of the mutant phenotype, the following stages and structures were scored in crosses between mutant females and wild-type males: (1) immediately after fertilization: yolk color, chorion elevation and softness, blastodisc formation; (2) at the 16-cell stage: morphology of blastomeres and the yolk cell; (3) during epiboly stages: morphology of yolk cytoplasm, blastomeres, germ ring and shield formation, migration of the yolk syncytial layer and enveloping layer. Mutant phenotypes first visible at 1 dpf were scored as described (Haffter et al., 1996). We staged oocytes as described (Selman et al., 1993).

Sperm Activation and In Vitro Fertilization

Sperm were collected, mounted on glass slides under a bridged coverslip, and activated by the addition of water. In vitro fertilization was performed as described (Dekens et al., 2003).

Whole-Mount In Situ Hybridization and Antibody Staining

Whole-mount in situ hybridization was carried out with probes for *no tail/brachyury* (Schulte-Merker et al., 1994), *cyclinB* (Kondo et al., 1997), and *bruno-like* (Suzuki et al., 2000). Antibody staining was done essentially as described (Dekens et al., 2003). Cortical granules were visualized with 50 μg/ml FITC conjugated MPA (*Maclura pomifera* agglutinin) as described (Becker and Hart, 1999). To visualize membranes, the yolk of the fixed embryos was removed after rehydration from methanol, and embryos were blocked in 1% BSA/PBST for at least 1 hr at room temperature and incubated in a 1:50 dilution of anti-β-catenin antibody (Schneider et al., 1996). The secondary antibody Alexa-Fluor 594 conjugated goat anti-rabbit (Molecular Probes) was used. All stainings were mounted in vectashield containing DAPI (Molecular Probes) and imaged on a Zeiss confocal microscope.

Genomic Mapping and PCR

Genomic DNA was isolated from tail fin clips, and mutant or wild-type sibling DNA was pooled for bulk segregant analysis. SSLP-markers were identified from the zebrafish genetic map (Shimoda et al., 1999), which were polymorphic in our mapping cross strains. PCR amplification was performed as follows: 95°C for 3 min; 35 to 40 cycles of 95°C for 15 s, 57°C for 15 s, 72°C for 30 s; final extension for 3 min. A subset of SSLP-primers were fluorescently labeled with FAM, HEX, or TET and the PCR-products separated on an ABI-Genescan analyzer. Conventional PCR products were analyzed on 3% agarose gels as described (Rauch et al., 1997).

The GFP-transgene in the fertilization assay was detected by PCR from genomic DNA was prepared from embryos, which were manually dechorionated at 3 hpf to eliminate sperm attached to the chorion. The primers used were forward: ACGTAAACGGCCACAAG TTCAG; reverse: TTACTTGTACAGCTCGTCCATGCCG.

Acknowledgments

We thank C. Howley and R. Ho for reagents, J.A. Campos-Ortega and C. Kimmel for the H2A::GFP fish line, F. Pelegri for communicating unpublished results, R. Geisler for a list of "first pass" SSLP-markers, our fish facility staff, and D. Cobb, B. Kilgore, C. Miller, D. Peterson, and B. Vought for assistance in the screen. We are grateful to M. Bartolomei, S. DiNardo, and M. Granato for valuable comments on the manuscript. K.A.M. coauthored this article in his private capacity. The views expressed in the article do not necessarily represent the views of the NIH, the DHHS, or the United States. This work was supported in part by research Grant No. 1-FY02-24 from the March of Dimes Birth Defects Foundation, NIH grant (ES11248) to M.C.M., DAAD-fellowship (Deutscher Akademischer Austauschdienst) to R.D., NRSA fellowship (F32-GM019803) to D.S.W., American Cancer Society fellowship (PF-98-037-01) to K.A.M., and NIH training program grant HD07516 to A.P.W.

Received: July 26, 2003
Revised: March 29, 2004
Accepted: March 29, 2004
Published: June 7, 2004

References

Bally-Cuif, L., Schatz, W.J., and Ho, R.K. (1998). Characterization of the zebrafish Orb/CPEB-related RNA-binding protein and localization of maternal components in the zebrafish oocyte. Mech. Dev. *77*, 31–47.

Becker, K.A., and Hart, N.H. (1999). Reorganization of filamentous actin and myosin-II in zebrafish eggs correlates temporally and spatially with cortical granule exocytosis. J. Cell Sci. *112*, 97–110.

Bourc'his, D., Xu, G.L., Lin, C.S., Bollman, B., and Bestor, T.H. (2001). Dnmt3L and the establishment of maternal genomic imprints. Science *294*, 2536–2539.

Burns, K.H., Viveiros, M.M., Ren, Y., Wang, P., DeMayo, F.J., Frail, D.E., Eppig, J.J., and Matzuk, M.M. (2003). Roles of NPM2 in chromatin and nucleolar organization in oocytes and embryos. Science *300*, 633–636.

Chen, S., and Kimelman, D. (2000). The role of the yolk syncytial layer in germ layer patterning in zebrafish. Development *127*, 4681–4689.

Christians, E., Davis, A.A., Thomas, S.D., and Benjamin, I.J. (2000). Maternal effect of Hsf1 on reproductive success. Nature *407*, 693–694.

Colledge, W.H., Carlton, M.B., Udy, G.B., and Evans, M.J. (1994). Disruption of c-mos causes parthenogenetic development of unfertilized mouse eggs. Nature *370*, 65–68.

Dekens, M.P., Pelegri, F.J., Maischein, H.M., and Nüsslein-Volhard, C. (2003). The maternal-effect gene *futile cycle* is essential for pronuclear congression and mitotic spindle assembly in the zebrafish zygote. Development *130*, 3907–3916.

De Robertis, E.M., Larrain, J., Oelgeschlager, M., and Wessely, O. (2000). The establishment of Spemann's organizer and patterning of the vertebrate embryo. Nat. Rev. Genet. *1*, 171–181.

Feldman, B., Gates, M.A., Egan, E.S., Dougan, S.T., Rennebeck, G., Sirotkin, H.I., Schier, A.F., and Talbot, W.S. (1998). Zebrafish organizer development and germ-layer formation require nodal-related signals. Nature *395*, 181–185.

Gurtu, V.E., Verma, S., Grossmann, A.H., Liskay, R.M., Skarnes, W.C., and Baker, S.M. (2002). Maternal effect for DNA mismatch repair in the mouse. Genetics *160*, 271–277.

Gardner, R.L. (2001). Specification of embryonic axes begins before cleavage in normal mouse development. Development *128*, 839–847.

Haffter, P., Granato, M., Brand, M., Mullins, M.C., Hammerschmidt, M., Kane, D.A., Odenthal, J., van Eeden, F.J., Jiang, Y.J., Heisenberg, C.P., et al. (1996). The identification of genes with unique and essential functions in the development of the zebrafish, *Danio rerio*. Development *123*, 1–36.

Hart, N.H. (1990). Fertilization in teleost fishes: mechanisms of sperm-egg interactions. Int. Rev. Cytol. *121*, 1–66.

Hart, N.H., and Fluck, R.A. (1995). Cytoskeleton in teleost eggs and early embryos: contributions to cytoarchitecture and motile events. Curr. Top. Dev. Biol. *31*, 343–381.

Hashimoto, N., Watanabe, N., Furuta, Y., Tamemoto, H., Sagata, N., Yokoyama, M., Okazaki, K., Nagayoshi, M., Takeda, N., Ikawa, Y., et al. (1994). Parthenogenetic activation of oocytes in c-mos-deficient mice. Nature *370*, 68–71.

Howell, C.Y., Bestor, T.H., Ding, F., Latham, K.E., Mertineit, C., Trasler, J.M., and Chaillet, J.R. (2001). Genomic imprinting disrupted by a maternal effect mutation in the Dnmt1 gene. Cell *104*, 829–838.

Howley, C., and Ho, R.K. (2000). mRNA localization patterns in zebrafish oocytes. Mech. Dev. *92*, 305–309.

Kimelman, D., and Kirschner, M. (1987). Synergistic induction of mesoderm by FGF and TGF-β and the identification of an mRNA coding for FGF in the early *Xenopus* embryo. Cell *51*, 869–877.

King, M.L., Zhou, Y., and Bubunenko, M. (1999). Polarizing genetic information in the egg: RNA localization in the frog oocyte. Bioessays *21*, 546–557.

Kondo, T., Yanagawa, T., Yoshida, N., and Yamashita, M. (1997). Introduction of cyclin B induces activation of the maturation-promoting factor and breakdown of germinal vesicle in growing zebrafish oocytes unresponsive to the maturation-inducing hormone. Dev. Biol. *190*, 142–152.

Leader, B., Lim, H., Carabatsos, M.J., Harrington, A., Ecsedy, J., Pellman, D., Maas, R., and Leder, P. (2002). Formin-2, polyploidy, hypofertility and positioning of the meiotic spindle in mouse oocytes. Nat. Cell Biol. *4*, 921–928.

Leung, C.F., Webb, S.E., and Miller, A.L. (2000). On the mechanism of ooplasmic segregation in single-cell zebrafish embryos. Dev. Growth Differ. *42*, 29–40.

Lincoln, A.J., Wickramasinghe, D., Stein, P., Schultz, R.M., Palko, M.E., De Miguel, M.P., Tessarollo, L., and Donovan, P.J. (2002). Cdc25b phosphatase is required for resumption of meiosis during oocyte maturation. Nat. Genet. *30*, 446–449.

Maegawa, S., Yasuda, K., and Inoue, K. (1999). Maternal mRNA localization of zebrafish DAZ-like gene. Mech. Dev. *81*, 223–226.

Mizuno, T., Yamaha, E., Wakahara, M., Kuroiwa, A., and Takeda, H. (1996). Mesoderm induction in zebrafish. Nature *383*, 131–132.

Moody, S.A., Bauer, D.V., Hainski, A.M., and Huang, S. (1996). Determination of *Xenopus* cell lineage by maternal factors and cell interactions. Curr. Top. Dev. Biol. *32*, 103–138.

Moon, R.T., and Kimelman, D. (1998). From cortical rotation to organizer gene expression: toward a molecular explanation of axis specification in *Xenopus*. Bioessays *20*, 536–545.

Mullins, M.C., Hammerschmidt, M., Haffter, P., and Nüsslein-Volhard, C. (1994). Large-scale mutagenesis in the zebrafish: in search of genes controlling development in a vertebrate. Curr. Biol. *4*, 189–202.

Nebreda, A.R., and Ferby, I. (2000). Regulation of the meiotic cell cycle in oocytes. Curr. Opin. Cell Biol. *12*, 666–675.

Ober, E.A., and Schulte-Merker, S. (1999). Signals from the yolk cell induce mesoderm, neuroectoderm, the trunk organizer, and the notochord in zebrafish. Dev. Biol. *215*, 167–181.

Pauls, S., Geldmacher-Voss, B., and Campos-Ortega, J.A. (2001). A zebrafish histone variant H2A.F/Z and a transgenic H2A.F/Z:GFP fusion protein for in vivo studies of embryonic development. Dev. Genes Evol. *211*, 603–610.

Payer, B., Saitou, M., Barton, S.C., Thresher, R., Dixon, J.P., Zahn, D., Colledge, W.H., Carlton, M.B., Nakano, T., and Surani, M.A. (2003). *stella* is a maternal effect gene required for normal early development in mice. Curr. Biol. *13*, 2110–2117.

Pelegri, F., and Schulte-Merker, S. (1999). A gynogenesis-based screen for maternal-effect genes in the zebrafish, *Danio rerio*. Methods Cell Biol. *60*, 1–20.

Pelegri, F., Knaut, H., Maischein, H.M., Schulte-Merker, S., and Nüsslein-Volhard, C. (1999). A mutation in the zebrafish maternal-effect gene nebel affects furrow formation and vasa RNA localization. Curr. Biol. *9*, 1431–1440.

Piotrowska, K., and Zernicka-Goetz, M. (2001). Role for sperm in spatial patterning of the early mouse embryo. Nature *409*, 517–521.

Postlethwait, J.H., and Talbot, W.S. (1997). Zebrafish genomics: From mutants to genes. Trends Genet. *13*, 183–190.

Rauch, G.J., Granato, M., and Haffter, P. (1997). A polymorphic zebrafish line for genetic mapping using SSLPs on high-percentage agarose gels. Trends Tech Tips Online *T01208*, http://tto.trends.-com/cgibin/tto/pr/pg.

Rebagliati, M.R., Toyama, R., Haffter, P., and Dawid, I.B. (1998). cyclops encodes a nodal-related factor involved in midline signaling. Proc. Natl. Acad. Sci. USA *95*, 9932–9937.

Sampath, K., Rubinstein, A.L., Cheng, A.H.S., Liang, J.O., Fekany, K., Solnica-Krezel, L., Korzh, V., Halpern, M.E., and Wright, C.V.E. (1998). Induction of the zebrafish ventral brain and floorplate requires cyclops/nodal signalling. Nature *395*, 185–189.

Schier, A.F. (2001). Axis formation and patterning in zebrafish. Curr. Opin. Genet. Dev. *11*, 393–404.

Schneider, S., Steinbeisser, H., Warga, R.M., and Hausen, P. (1996). Beta-catenin translocation into nuclei demarcates the dorsalizing centers in frog and fish embryos. Mech. Dev. *57*, 191–198.

Schulte-Merker, S., Hammerschmidt, M., Beuchle, D., Cho, K.W., De Robertis, E.M., and Nüsslein-Volhard, C. (1994). Expression of zebrafish goosecoid and no tail gene products in wild-type and mutant no tail embryos. Development *120*, 843–852.

Schultz, R.M. (1993). Regulation of zygotic gene activation in the mouse. Bioessays *15*, 531–538.

Selman, K., Wallace, R.A., Sarka, A., and Qi, X. (1993). Stages of oocyte development in the zebrafish, *Brachydanio rerio*. J. Morphol. *218*, 203–224.

Shimoda, N., Knapik, E.W., Ziniti, J., Sim, C., Yamada, E., Kaplan, S., Jackson, D., de Sauvage, F., Jacob, H., and Fishman, M.C. (1999). Zebrafish genetic map with 2000 microsatellite markers. Genomics *58*, 219–232.

Solnica-Krezel, L., Schier, A.F., and Driever, W. (1994). Efficient recovery of ENU-induced mutations from the zebrafish germline. Genetics *136*, 1401–1420.

Streisinger, G., Walker, C., Dower, N., Knauber, D., and Singer, F. (1981). Production of clones of homozygous diploid zebra fish (*Brachydanio rerio*). Nature *291*, 293–296.

Sullivan, W., Fogarty, P., and Theurkauf, W. (1993). Mutations affecting the cytoskeletal organization of syncytial *Drosophila* embryos. Development *118*, 1245–1254.

Suzuki, H., Maegawa, S., Nishibu, T., Sugiyama, T., Yasuda, K., and Inoue, K. (2000). Vegetal localization of the maternal mRNA encoding an EDEN-BP/Bruno-like protein in zebrafish. Mech. Dev. *93*, 205–209.

Tay, J., and Richter, J.D. (2001). Germ cell differentiation and synaptonemal complex formation are disrupted in CPEB knockout mice. Dev. Cell *1*, 201–213.

Tong, Z.B., Gold, L., Pfeifer, K.E., Dorward, H., Lee, E., Bondy, C.A., Dean, J., and Nelson, L.M. (2000). Mater, a maternal effect gene required for early embryonic development in mice. Nat. Genet. *26*, 267–268.

Wagner, D.S., Dosch, R., Mintzer, K.A., Wiemelt, A.P., and Mullins, M.C. (2004). Maternal control of development at the midblastula transition and beyond: mutants from the zebrafish II. Dev. Cell *6*, this issue, 781–790.

Wu, X., Viveiros, M.M., Eppig, J.J., Bai, Y., Fitzpatrick, S.L., and Matzuk, M.M. (2003). Zygote arrest 1 (*Zar1*) is a novel maternal-effect gene critical for the oocyte-to-embryo transition. Nat. Genet. *33*, 187–191.

Yang, J., Tan, C., Darken, R.S., Wilson, P.A., and Klein, P.S. (2002). β-Catenin/Tcf-regulated transcription prior to the midblastula transition. Development *129*, 5743–5752.